

# IceCube: the Discovery of High-Energy Cosmic Neutrinos

---

**Markus Ahlers and Francis Halzen**\* †

*University of Wisconsin–Madison, Madison, WI*

*E-mail:* [halzen@icecube.wisc.edu](mailto:halzen@icecube.wisc.edu)

Developments in neutrino astronomy have been to a great extent motivated by the search for the sources of cosmic rays, leading at an early stage to the concept of a cubic-kilometer neutrino detector. Four decades later, IceCube, taking data since 2012, has discovered a flux of high-energy neutrinos of cosmic origin consisting of tens of events with energies above 100 TeV. Among these are three with deposited energies of more than one PeV, the highest energy neutrinos ever detected. We will describe the instrument and its performance that made this discovery possible by measuring the energy of neutrinos that interact inside the instrumented volume. The observation has been confirmed by an independent analysis measuring the flux of high-energy secondary muons initiated by neutrinos reaching the detector from below. The origin of the neutrinos is at this point unclear. Because of the extraordinary transparency of the natural ice, a telescope with an instrumented volume on the order of 10 km<sup>3</sup> and an adequate, though higher, energy threshold can be constructed by only doubling the IceCube instrumentation.

*Frontiers of Fundamental Physics 14 - FFP14,*

*15-18 July 2014*

*Aix Marseille University (AMU) Saint-Charles Campus, Marseille*

---

\*Speaker.

†Discussion with collaborators inside and outside the IceCube Collaboration, too many to be listed, have greatly shaped this presentation. Thanks. This research was supported in part by the U.S. National Science Foundation under Grants No. ANT-0937462 and PHY-1306958 and by the University of Wisconsin Research Committee with funds granted by the Wisconsin Alumni Research Foundation.

## 1. IceCube: the First Kilometer-Scale Neutrino Detector

Soon after the 1956 observation of the neutrino [1], the idea emerged that it represented the ideal astronomical messenger [2, 3, 4]. The concept has since been demonstrated: neutrino detectors have “seen” the Sun and detected a supernova in the Large Magellanic Cloud in 1987. Both observations were of tremendous importance; the former showed that neutrinos have a tiny mass, opening the first chink in the armor of the Standard Model of particle physics, and the latter confirmed the basic nuclear physics of the death of stars.

High-energy neutrinos have a distinct potential to probe the extreme Universe. Neutrinos reach us from the edge of the Universe without absorption and with no deflection by magnetic fields. They can escape unscathed from the inner neighborhood of black holes and from the accelerators where cosmic rays are born. Their weak interactions also make neutrinos very difficult to detect. Immense particle detectors are required to collect cosmic neutrinos in statistically significant numbers [5]. Already by the 1970s, it had been understood [6] that a kilometer-scale detector was needed to observe the “cosmogenic” neutrinos produced in the interactions of cosmic rays with background microwave photons [7]. Today’s estimates of the sensitivity for observing potential cosmic ray accelerators such as Galactic supernova remnants, active galactic nuclei (AGN), and  $\gamma$ -ray bursts (GRB) unfortunately point to the same exigent requirement [5]. Building a neutrino telescope has been a daunting technical challenge.

Given the detector’s required size, early efforts concentrated on instrumenting large volumes of natural water with photomultipliers that detect the Cherenkov light emitted by the secondary particles produced when neutrinos interact with nuclei inside or near the detector [8]. After a two-decade-long effort, building the Deep Underwater Muon and Neutrino Detector (DUMAND) in the sea off the main island of Hawaii unfortunately failed [9]. However, DUMAND pioneered many of the detector technologies in use today and inspired the deployment of a smaller instrument in Lake Baikal [10] as well as efforts to commission neutrino telescopes in the Mediterranean [11, 12, 13]. These have paved the way toward the planned construction of KM3NeT [14]. The first telescope on the scale envisaged by the DUMAND collaboration was realized instead by transforming a large volume of deep Antarctic ice into a particle detector, the Antarctic Muon and Neutrino Detector Array (AMANDA). In operation from 2000 to 2009, it represented the proof of concept for the kilometer-scale neutrino observatory, IceCube [15, 16], completed in 2010.

The IceCube neutrino detector (Fig. 1) consists of 86 strings, each instrumented with 60 ten-inch photomultipliers spaced 17 m apart over a total length of one kilometer. The deepest modules are located at a depth of 2.45 km so that the instrument is shielded from the large background of cosmic rays at the surface by approximately 1.5 km of ice. Strings are arranged at apexes of equilateral triangles that are 125 m on a side. The instrumented detector volume is a cubic kilometer of dark and highly transparent [17] Antarctic ice.

Each digital optical module (DOM) consists of a glass sphere containing the photomultiplier and the electronics board that digitizes the signals locally using an onboard computer. The digitized signals are given a global time stamp with residuals accurate to less than 3 ns and are subsequently transmitted to the surface. Processors at the surface continuously collect the time-stamped signals from the optical modules, each of which functions independently. The digital messages are sent to a string processor and a global event builder. They are subsequently sorted into the Cherenkov

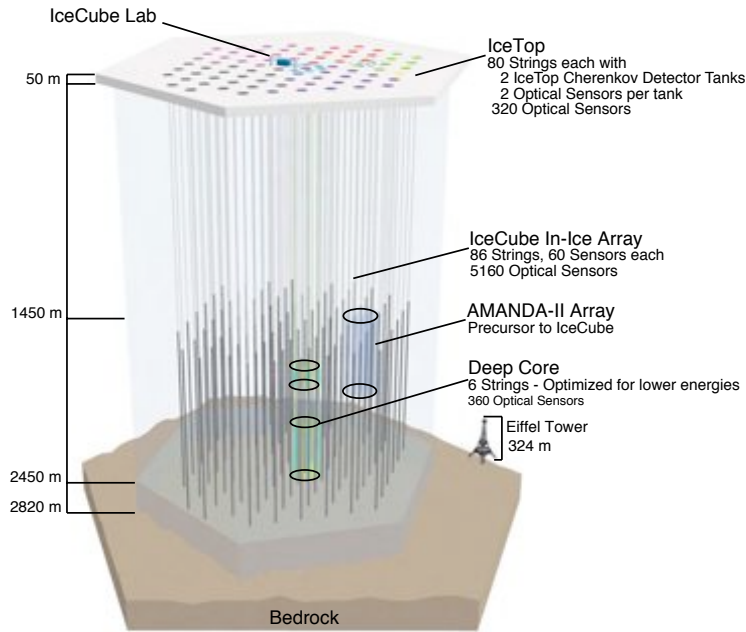


**Figure 1:** Sketch of the IceCube observatory.

patterns emitted by secondary muon tracks, or electron and tau showers, that reveal the direction of the parent neutrino [18].

The depth of the detector and its projected area determine the trigger rate of approximately 3 kHz for penetrating muons produced by interactions of cosmic rays in the atmosphere above. The ratio of neutrino-induced signal to atmospheric background is on the order of one per million at TeV energy. The neutrino rate is dominated by neutrinos produced in the Earth's atmosphere. The first challenge is to select a sufficiently pure sample of neutrinos, and the second is to identify the small fraction that are astrophysical in origin.

Neutrino events may be broadly classified in two groups, muon tracks and particle showers (cascades), which reflect the patterns of Cherenkov light emitted by the charged particles produced when the neutrinos interact. Tracks are produced by charged current interactions of muon neutrinos while cascades are produced by charged current interactions of electron and tau neutrinos as well as neutral current interactions of all flavors. The travel range for  $\nu_\mu$ -induced muons is on the order of kilometers, while the length scale characteristic of the electromagnetic showers that dominate the cascade events is only tens of meters. Another way to classify neutrino events is to distinguish events that start inside the detector from those in which the neutrino interacts outside the detector. The largest neutrino sample consists of  $\nu_\mu$ -induced muons entering the detector from zenith angles too large to be atmospheric in origin, typically  $\theta \geq 85^\circ$ . The rate of such events in the full IceCube detector is approximately 100 per day or more, depending on how the threshold for a particular analysis is set. The mean energy of this sample, dominated by atmospheric neutrinos, is  $1 \sim 10$  TeV.

By specializing to events starting inside the detector, one instead observes neutrinos of all flavors. For  $E_\nu < 1$  PeV the interaction of a  $\nu_\tau$  in IceCube will look much like that of a  $\nu_e$  because the track length of the  $\nu_\tau$  of less than 50 m is smaller than the 125 m string spacings and difficult to

identify. Analysis techniques are under development to remedy this.

Reconstruction of events depends on accurate timing ( $< 3$  ns) and on the ability to measure the amount of Cherenkov light generated along the tracks of charged particles produced by the neutrino interactions. Basically, the arrival time of photons at the DOMs determines the trajectory and the amount of light determines the deposited energy. The number of photons produced per unit of path length and their distribution in wavelength are well-known quantities [19]. A detailed understanding of the properties of the propagation of the photons in the ice [17] is crucial to relate light generated to light observed in the DOMs. Reconstruction of tracks in ice has been well studied [20]. For typical kilometer tracks, the angular resolution is better than  $0.4^\circ$ . Reconstruction of cascade events is a topic of current study in IceCube [21]. Determining the deposited energy from the observed light pool is relatively straightforward, and a resolution of better than 15 % is possible; the same value holds for the reconstruction of the energy deposited by a muon track inside the detector. The angular resolution for cascades is significantly poorer than for tracks. In the large cascades studied by detailed simulations on an event-by-event basis, it is possible to determine the directions to within  $15^\circ$  based on shapes of the photon timing patterns in each DOM, which reflect the directionality of the cascade electrons.

Atmospheric neutrinos are a background for cosmic neutrinos, at least at energies below  $\sim 100$  TeV. Above this energy, their flux is too small to produce events in a kilometer-scale detector and every event is a discovery. This is how IceCube made its initial observation of cosmic neutrinos.

## 2. Neutrinos Associated with Cosmic Rays

Despite their discovery potential touching a wide range of scientific issues, from the search for dark matter to the study of neutrinos themselves, the construction of kilometer-scale neutrino detectors has been largely motivated by the prospect of detecting neutrinos associated with cosmic ray sources. Cosmic accelerators produce particles with energies in excess of 100 EeV; we still do not know where or how this occurs [22]. The bulk of the cosmic rays are Galactic in origin. Any association with our Galaxy presumably disappears at EeV energy when the gyroradius of a proton in the Galactic magnetic field exceeds its size. The cosmic-ray spectrum exhibits a rich structure above an energy of  $\sim 0.1$  EeV, but where exactly the transition to extragalactic cosmic rays occurs is a matter of debate.

Speculations on the origin of cosmic rays generally agree on the fact that the power of the accelerator is supplied by the gravitational energy of a collapsed object: supernova remnants in our Galaxy and  $\gamma$ -ray bursts, starbursts, and active galaxies throughout the Universe. The detailed blueprint for a cosmic-ray accelerator must meet two challenges: the highest energy particles in the beam must reach beyond  $10^3$  TeV ( $10^8$  TeV) for Galactic (extragalactic) sources, and their luminosities must be able to accommodate the observed flux. Both requirements represent severe constraints that have, with some exceptions, focused theoretical speculations on these source candidates.

Neutrinos are produced in association with the cosmic-ray beam. Cosmic rays accelerated in regions of high magnetic fields near black holes or neutron stars inevitably interact with radiation surrounding them. In particle physics language; cosmic-ray accelerators are beam dumps. In supernova shocks, cosmic rays inevitably interact with the hydrogen in the Galactic disk, producing

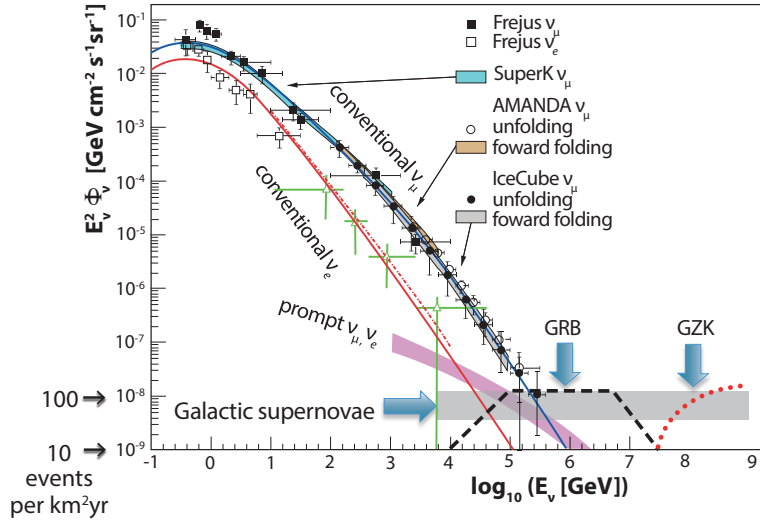


**Figure 2:** Anticipated cosmic-neutrino fluxes produced by supernova remnants and GRBs exceed the atmospheric neutrino flux in IceCube above 100 TeV because of their relatively soft  $E^{-2}$  high-energy spectrum. (Note that the flux has been multiplied by a factor of  $E^2$ ). Also shown is a sample calculation of the cosmogenic neutrino flux. The atmospheric electron-neutrino spectrum (green open triangles) is from [17]. The conventional  $\nu_e$  (red line) and  $\nu_\mu$  (blue line) from Honda,  $\nu_e$  (red dotted line) from Bartol and charm-induced neutrinos (magenta band) [23] are shown. Previous measurements from Super-K [24], Frejus [25], AMANDA [26, 27] and IceCube [28, 29] are also shown.

equal numbers of pions of all three charges that decay into pionic photons and neutrinos. Their secondary fluxes should be boosted by the interaction of the cosmic rays with high-density molecular clouds that are ubiquitous in the star-forming regions where supernovae are more likely to explode. For extragalactic sources, the neutrino-producing target may be light, for instance photons radiated by the accretion disk of an AGN or synchrotron photons that coexist with protons in the expanding fireball producing a GRB.

Estimating the neutrino flux associated with cosmic rays accelerated in supernova remnants and GRBs is relatively straightforward as both the beam, identified with the observed cosmic-ray flux, and the targets, observed by astronomers, are known. The resulting estimates are shown in Fig. 2. Although subject to astrophysical uncertainties, the message is clear, neutrinos from cosmic-ray accelerators dominate the steeply falling atmospheric neutrino flux above an energy of  $\sim 100$  TeV. The estimates shown assumed a  $E^{-2}$  dependence typical of what is observed for non-thermal sources of high-energy  $\gamma$ -rays. The anticipated level of events observed in a cubic-kilometer neutrino detector is  $10 \sim 100$  per year. These estimates reinforced the logic for building a cubic kilometer neutrino detector. A more detailed description of the theoretical estimates can be found in reference [18].

If collapsing stars are the origin of cosmic rays as is the case for supernova remnants, GRBs, and starburst galaxies, it is reasonable to expect [30] that IceCube should observe neutrinos from

the nearby star-forming region in Cygnus. With a probability of only 2% at this point, the excess observed in the IceCube four-year search for point sources in this region is nevertheless interesting [31].

### 3. Discovery of Cosmic Neutrinos

The generation of underground neutrino detectors preceding construction of the AMANDA detector searched for cosmic neutrinos without success and established an upper limit on their flux, assuming an  $E^{-2}$  energy dependence [32]:

$$E_\nu^2 \frac{dN}{dE_\nu} \leq 5 \times 10^{-9} \text{TeV cm}^{-2} \text{s}^{-1} \text{sr}^{-1} \quad (3.1)$$

Operating for almost one decade, the AMANDA detector improved this limit by two orders of magnitudes. With data taken during its construction, IceCube's sensitivity rapidly approached the theoretical flux estimates for candidate sources of cosmic rays such as supernova remnants,  $\gamma$ -ray bursts and, with a larger uncertainty, active galactic nuclei; see Fig. 2. With its completion, IceCube also positioned itself for observing the much anticipated flux of cosmogenic neutrinos, with some estimates predicting as many as two events per year.

Cosmogenic neutrinos were the target of a dedicated search using IceCube data collected between May 2010 and May 2012. Two events were found [33]. However, their energies, rather than EeV, as expected for cosmogenic neutrinos, were in the PeV range: 1,040 TeV and 1,140 TeV. The events are particle showers initiated by neutrinos interacting inside the instrumented detector volume. Their light pool of roughly one hundred thousand photoelectrons extends over more than 500 meters; see Fig. 3. With no evidence of a muon track, they are initiated by electron or tau neutrinos.

Previous to this serendipitous discovery, neutrino searches had almost exclusively specialized to the observation of muon neutrinos that interact primarily outside the detector to produce kilometer-long muon tracks passing through the instrumented volume. Although creating the opportunity to observe neutrinos interacting outside the detector, it is necessary to use the Earth as a filter to remove the huge background flux of muons produced by cosmic ray interactions in the atmosphere. This limits the neutrino view to a single flavor and half the sky. Inspired by the observation of the two PeV events, a filter was designed that exclusively identifies neutrinos interacting inside the detector. It divides the instrumented volume of ice into an outer veto shield and a 420 megaton inner fiducial volume. The separation between veto and signal regions was optimized to reduce the background of atmospheric muons and neutrinos to a handful of events per year while keeping 98% of the signal. The great advantage of specializing to neutrinos interacting inside the instrumented volume of ice is that the detector functions as a total absorption calorimeter measuring energy with a 10–15% resolution. Also, neutrinos from all directions in the sky can be identified, including both muon tracks produced in  $\nu_\mu$  charged-current interactions and secondary showers produced by neutrinos of all flavors.

Analyzing the data covering the same time period as the cosmogenic neutrino search, 28 candidate neutrino events were identified with in-detector deposited energies between 30 and 1140 TeV; see Fig. 4. Of these, 21 are showers whose energies are measured to better than 15% but

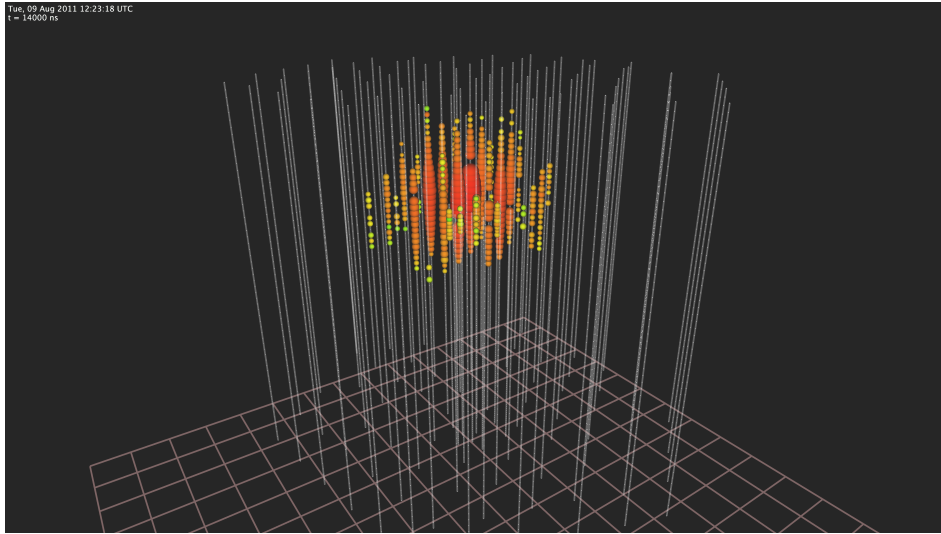


**Figure 3:** Light pool produced in IceCube by a high-energy neutrino. The measured energy is 1.04 PeV, which represents a lower limit on the energy of the neutrino that initiated the shower. The vertical lines of white dots represent the sensors that report any detected signal. Color of the dots indicates arrival time, from red (early) to purple (late) following the rainbow. Size of the dots indicates the number of photons detected.

whose directions are determined to 10-15 degrees only. Predominantly originating in the Southern Hemisphere, none show evidence for a muon track. If atmospheric in origin, the neutrinos should be accompanied by muons produced in the air shower in which they originate. For example, at 1 PeV, less than 0.1% of atmospheric showers contain no muons with energy above 500 GeV, approximately that which is needed to reach the detector in the deep ice when traveling vertically.

The remaining seven events are muon tracks, which do allow for subdegree angular reconstruction; only a lower limit on their energy can be established because of the unknown fraction carried away by the exiting muon track. Furthermore, with the present statistics, these are difficult to separate from the competing atmospheric background. The 28 events include the two PeV events previously revealed in the cosmogenic neutrino search. The signal of 28 events on an atmospheric background of  $10.6^{+5.0}_{-3.6}$  represents an excess over background of more than 4 standard deviations.

The large errors on the background are associated with the possible presence of a neutrino component originating from the production and prompt leptonic decays of charmed particles in the atmosphere. Such a flux has not been observed so far. While its energy and zenith angle dependence are known, its normalization is not; see Fig. 2 for one attempt at calculating the flux of charm origin. Neither the energy, nor the zenith angle dependence of the 28 events observed can be described by a charm flux, and, in any case, fewer than 3.4 events are allowed at the  $1\sigma$  level by the present upper limit on a charm component of the atmospheric flux set by IceCube itself [34]. As already mentioned, in the case of a charm origin, the excess events should contain accompanying muons from the atmospheric shower that produced them, but they do not.

Fitting the data to a superposition of extraterrestrial neutrinos on an atmospheric background

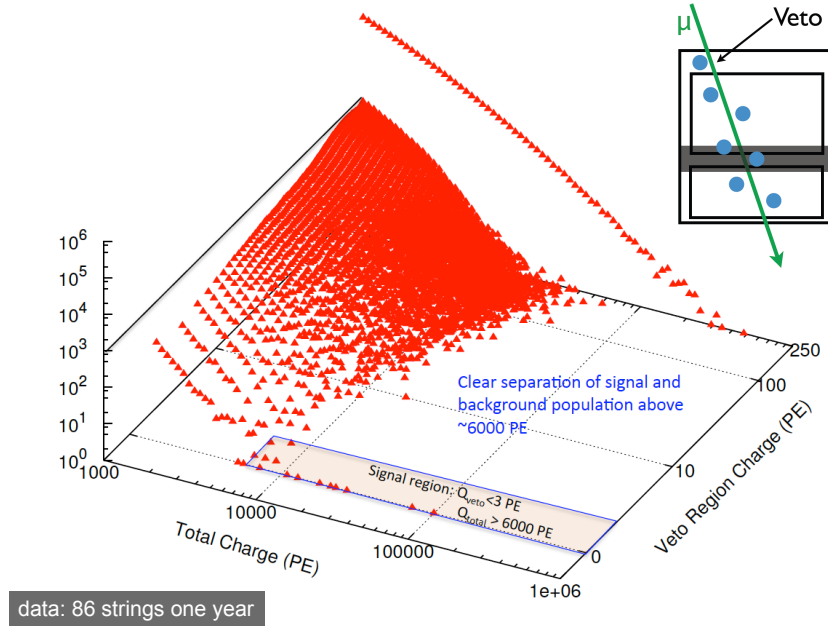


**Figure 4:** One year of IceCube data from its final 86-string configuration showing number of events as a function of the total number of photoelectrons and the number present in the veto region. The signal region requires more than 6000 photoelectrons with less than three of the first 250 in the veto region of the detector. The signal, including nine events with reconstructed neutrino energy in excess of 100 TeV, is clearly separated from the background.

yields a cosmic neutrino flux of

$$E_\nu^2 \frac{dN}{dE_\nu} = 3.6 \times 10^{-11} \text{ TeV cm}^{-2} \text{ s}^{-1} \text{ sr}^{-1} \quad (3.2)$$

for the sum of the three neutrino flavors. As discussed in section 2, this is the level of flux anticipated for neutrinos accompanying the observed cosmic rays. Also, the energy and zenith angle dependence observed is consistent with what is expected for a flux of neutrinos produced by cosmic accelerators; see Figs. 5 and 6. The flavor composition of the flux is, after corrections for the acceptances of the detector to the different flavors, consistent with 1:1:1 as anticipated for a flux originating in cosmic sources.

Clearly, the major uncertainty in the spectrum of atmospheric neutrinos at high energy is the level of charm production. The short-lived charmed hadrons preferentially decay up to a characteristic energy of  $10^7$  GeV, producing prompt muons and neutrinos with the same spectrum as their parent cosmic rays. This prompt flux of leptons has not yet been measured. Fits to both starting-event and upgoing muon-neutrino-data samples prefer a vanishing charm component. Existing limits [36, 37] allow a charm component at a level predicted by a dipole model calculation for the high-energy charm cross section [23]. In this context, it is important to point out that the muon produced in the same decay as the neutrino is guaranteed to reach the detector for muon neutrinos from above when the neutrino energy is sufficiently high and the zenith angle sufficiently small

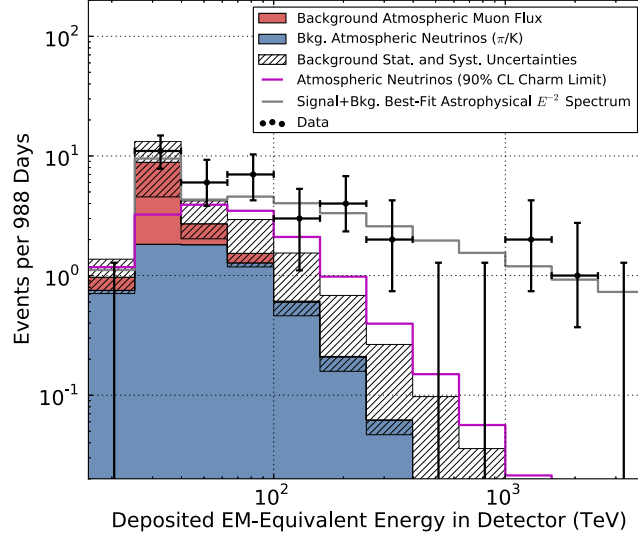


**Figure 5:** Deposited energies of events observed in three years of data with predictions. The hashed region shows uncertainties on the sum of all backgrounds. Muons (red) are computed from simulation to overcome statistical limitations in our background measurement and scaled to match the total measured background rate. Atmospheric neutrinos and uncertainties thereon are derived from previous measurements of both the  $\pi, K$  and charm components of the atmospheric spectrum [35]. A gap larger than the one between 400 and 1000 TeV appears in 43% of realizations of the best-fit continuous spectrum.

[38]. In this case, the atmospheric neutrino provides its own self-veto. This self-veto has been applied to the data sample and further suppresses any potential charm component.

#### 4. Confirmation of a Cosmic Component of the Neutrino Spectrum

Two additional years of data have been taken with the completed detector, and the first of these has been analyzed [39]. Using identical methods, the third year (2012-2013) of data yields results that are consistent with those described above. In combining the three years of data, a purely atmospheric explanation can be excluded at  $5.7\sigma$ . The three-year data set, with a livetime of 988 days, contains a total of 36 neutrino candidate events with deposited energies ranging from 30 to 2000 TeV. The 2000 TeV event is the highest energy neutrino interaction ever observed. Note that Figs. 5 and 6 show the three-year sample.

Additionally, a totally independent analysis of the spectrum of muon neutrinos passing through the Earth has confirmed the existence of an astrophysical component first observed in neutrino events interacting inside the detector. Because of their significantly harder energy spectrum, a flux of astrophysical neutrinos as observed in the starting-event analysis should populate, in fact dominate, the spectrum of muon-induced neutrinos beyond the steepening atmospheric flux. The spectrum of the atmospheric neutrino background becomes indeed one power steeper than the spectrum of primary cosmic rays at high energy as the competition between interaction and decay of pions and kaons increasingly suppresses their decay. A further steepening occurs above 100 TeV as a consequence of a steepening in the primary spectrum, the so-called “knee.” As already discussed,

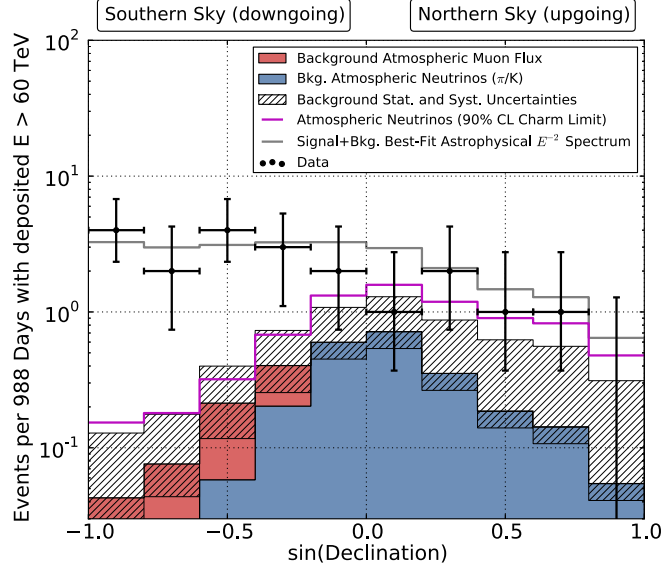


**Figure 6:** Arrival angles of events with  $E_{dep} > 60$  TeV. The increasing opacity of the Earth to high-energy neutrinos suppresses the signal to the right of the plot. Vetoing atmospheric neutrinos by muons from their parent air showers depresses the atmospheric neutrino background on the left. The data are described well by an astrophysical isotropic  $E^{-2}$  spectrum with a normalization of  $E_{\nu}^2 \frac{dN}{dE_{\nu}} = 0.95 \pm 0.3 \times 10^{-8} \text{ GeV cm}^{-2} \text{ s}^{-1} \text{ sr}^{-1}$  for a single flavor, assuming equal contributions of all 3 flavors.

atmospheric neutrino events with energies exceeding 100 TeV are therefore rare, on the order of one event per year even in a detector the size of IceCube.

An analysis of the same two years of data used for the starting-event analysis has revealed an excess of high-energy  $\nu_{\mu}$ -induced muons penetrating the Earth from the Northern Hemisphere [40]. Their spectrum is consistent with the one obtained in the starting event analysis; see Fig. 7. Shown is the muon neutrino flux as a function of the energy deposited by the muons inside the detector. This reflects the energy of the neutrino that initiated the events; for instance, the highest energies in Fig. 7 correspond, on average, to parent neutrinos of PeV energy. A best fit to the spectrum that includes a conventional, charm and astrophysical component with free normalizations yields the results shown in the figure.

## 5. Neutrino Stars?

Where do the cosmic neutrinos originate? Figure 8 shows the arrival directions of the three-year starting-event sample in Galactic coordinates in terms of cascade events (filled circles) and track events (diamonds). The deposited energy is indicated by the size of the symbols. In the case of the cascades, we indicate the angular reconstruction error by thin circles. We also indicate the minimum (30 TeV) neutrino in-Earth absorption as 10% quantiles. The absorption effect of neutrinos (and background muons) in the Northern Hemisphere is clearly visible in the event distribution. Anisotropy studies of the arrival directions of these events account for this bias via background maps that are obtained from right ascension scrambling of events.

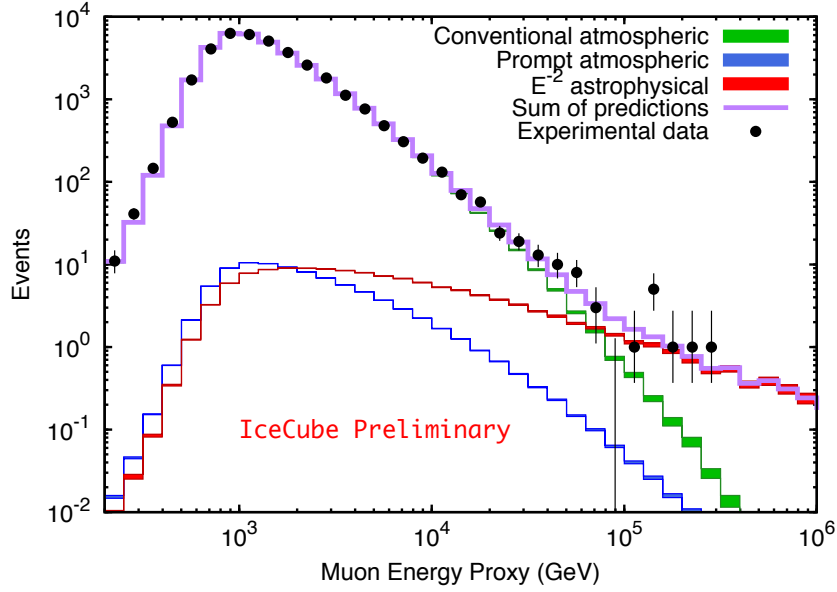


**Figure 7:** Spectrum of secondary muons initiated by muon neutrinos that have traversed the Earth, i.e., with zenith angle less than  $5^\circ$  above the horizon, as a function of the energy they deposit inside the detector. The highest energy muons are, on average, initiated by PeV neutrinos.

No significant local excess in the sky was found when compared to these randomized pseudoexperiments. Repeating the analysis for showers only, a hot spot appears close to the Galactic center. After correcting for trials, the probability of it emerging from background is 7.2%. Correlation with the Galactic plane is also not significant: when letting the width float freely, the best fit returned a value of  $7.5^\circ$  with a post-trial chance probability of 2.8%. The high Galactic latitudes of some of the high-energy events suggest an extragalactic component at some level. We also searched for clustering of the events in time and investigated a possible correlation with the times of observed GRBs. No statistically significant correlation was found.

At this point, the events are consistent with a diffuse flux of neutrinos equally distributed between the three flavors. For instance, if the cluster of eight events within  $30^\circ$  of the Galactic center, referred to above, originated from a point source, the corresponding expected flux would be  $E_\nu^2 dN_{\nu_\mu + \bar{\nu}_\mu} / dE_\nu \simeq 6 \times 10^{-11} \text{ TeV cm}^{-2} \text{ s}^{-1}$ , yielding 45 events per year. This flux is simply estimated by multiplying the diffuse flux by  $4\pi \times 8 / (36 - 15)$ , where we corrected for the number of about 15 background events in the sample of 36. The number is not corrected for the fact that the center of the Galaxy is only visible 68% of the time for a Mediterranean detector. In any case, any strong point source in the Northern Hemisphere should not have escaped detection in the dedicated searches performed by IceCube and ANTARES [41], reinforcing the evidence that we are most likely detecting a flux of a relatively large number of relatively weak sources. For extended sources, this conclusion can be evaded as the sensitivity level increases with the ratio of angular size to angular resolution for background-dominated event samples.

Importantly, note that the highest energy events in Fig. 7 represent a sample of tens of muon neutrinos with very little background. These have been reconstructed with  $0.4^\circ$  resolution, which can be improved upon off-line. Though clustered around the horizon where the Earth is transparent

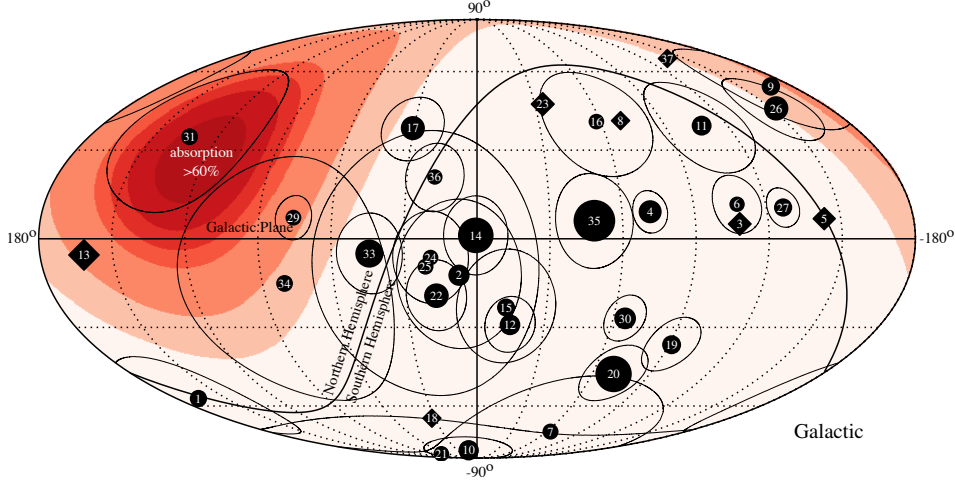


**Figure 8:** Arrival directions of events of the three-year starting-event sample in Galactic coordinates. Shower-like events are shown with filled circles and those containing muon tracks with diamonds. The size of the symbols indicates the deposited energy of the events in the range of 30 TeV to 2 PeV. The thin circles around cascade events indicate the angular reconstruction uncertainty. The red-shaded regions show 10% quantiles of neutrino in-Earth absorption at 30 TeV and increasing with neutrino energy. Note that the track-like event 28 has been omitted following the discussion in Ref. [39].

to PeV-energy neutrinos, the search for the sources using this sample is likely to be more promising. For additional information, see [42].

If cosmic accelerators are the origin of the observed flux, then the neutrinos have been produced in proton-photon ( $p\gamma$ ) or proton-proton ( $pp$ ) interactions with radiation or gas at the acceleration site or along the path traveled by cosmic rays to Earth. The fraction of energy transferred to pions is about 20% and 50% for  $p\gamma$  and  $pp$ , respectively, and each of the three neutrinos from the decay chain  $\pi^+ \rightarrow \mu^+ \nu_\mu$  and  $\mu^+ \rightarrow e^+ \nu_e \bar{\nu}_\mu$  carries about one quarter of the pion energy. Hence, the cosmic rays producing the excess neutrinos have energies of tens of PeV, well above the knee in the spectrum. It is tantalizingly close to the energy of 100 PeV [43, 44] where the spectrum displays a rich structure. While these cosmic rays are commonly categorized as Galactic, with the transition to the extragalactic population at the ankle in the spectrum at  $3 \sim 4$  EeV, one cannot rule out a subdominant contribution of PeV neutrinos of extragalactic origin. IceCube neutrinos may give us information on the much-debated transition energy.

It is also interesting that the observed flux level in Eq.(3.2) saturates a limit on neutrino fluxes associated with the sources of ultra-high-energy (UHE) cosmic rays [45, 46]. This limit considers the fact that the (time-integrated) energy density of neutrinos cannot exceed the energy density of the intrinsic flux of UHE CRs. The CR energy density of the sources can be estimated from the observed CR spectrum, assuming that the sources are transparent to UHE CRs. If the observed fluxes of neutrinos and UHE CRs are indeed related, it requires the sources to be operating close to the calorimetric limit [47] with efficient neutrino production. The sum of all calorimetric UHE CR sources would then naturally explain the observation [48].

Whether of  $pp$  or  $p\gamma$  origin, neutrinos are accompanied by  $\gamma$ -rays that are the decay products of neutral pions produced in association with the charged ones. The intrinsic  $\gamma$ -ray flux on production is simply related to the observed neutrino flux and has a weak dependence on the ratio of charged to neutral pions in  $pp$  and  $p\gamma$  interactions; see, e.g., Ref. [49]. Direct observation of  $\gamma$ -rays corresponding to neutrino emission in the 10-TeV to PeV range is, however, only possible for close-by emission due to the  $\gamma$ -ray opacity of the Universe. In particular, PeV photons can only reach us from Galactic distances as large as 10 kpc with modest attenuation.

In fact, the  $\gamma$ -ray flux accompanying Eq. 3.2 is in conflict with the diffuse upper limits of the CASA-MIA [50, 51] and KASCADE [52] experiments. This apparently disfavors the Galactic origin of the IceCube flux [49]. This conclusion does, however, depend on the assumption that the sources are transparent to  $\gamma$ -rays and that the flux is isotropic. Specifically, Galactic origin cannot be ruled out for subclasses of events like the previously mentioned cluster of events near the Galactic center. However, all experiments besides IceCube are in the Northern Hemisphere, leaving a blind spot in the sky at declination range  $-60^\circ < \delta < -20^\circ$  that contains about half of the IceCube events [49].

If, in fact, any of the IceCube events observed in the blind spot do originate from a Galactic source, IceCube itself should be able to observe the accompanying PeV  $\gamma$ -rays [53]. These are detected as muon-poor showers triggered by IceTop. The present limit on diffuse emission in the IC-40 FoV (zenith angle  $\lesssim 30^\circ$ ) is on the order of  $7 \times 10^{-8} \text{ GeV cm}^{-2} \text{ s}^{-1} \text{ sr}^{-1}$  [49], which is only a factor of 2–3 larger than the (unattenuated)  $\gamma$ -ray emission associated with the diffuse neutrino flux (3.2). The full IceCube observatory with an extended FoV (zenith angle  $\lesssim 40^\circ$ ) and increased exposure is even more sensitive to a local (quasi-)isotropic production of PeV neutrinos, e.g., neutrino production in the Galactic halo or PeV dark matter decay in the Galaxy [49].

If, on the other hand, the flux emerges from extragalactic sources, the direct observation of 10-TeV to PeV  $\gamma$ -rays is not possible. Instead,  $\gamma$ -rays in this energy range initiate electromagnetic cascades via repeated  $\gamma\gamma$  pair production with cosmic radiation backgrounds and inverse Compton scattering of electrons and positrons. This is a calorimetric process that shifts the integrated energy of  $\gamma$ -rays into the sub-TeV region. Here, the observation of a diffuse  $\gamma$ -ray background with Fermi LAT can serve as an additional constraint [54]. This secondary emission is presently marginally consistent with the observation, but it could become important in the case that future  $\gamma$ -ray observations reduce the background by the identification of additional sources.

For  $pp$  production of  $\gamma$ -rays and neutrinos, we can utilize the fact that the emission spectrum is expected to follow a simple power law inherited from the initial cosmic-ray spectrum that extends to energies on the order of GeV. In this case, the Fermi LAT background sets an upper limit on the low-energy extension of direct photons associated with the IceCube observation [55]. The sum of direct and indirect photons requires the spectral index of the observation to be softer than  $\gamma \simeq 2.2$ . If future neutrino observations with better statistics require a softer index this would favor a  $p\gamma$  origin of the emission, or it would imply that the corresponding source population has already been identified via their sub-TeV  $\gamma$ -ray emission.

In summary, evidence seems to point to a diffuse flux of relatively weak sources most likely of extragalactic origin. A Galactic component cannot be excluded. The sample of events is simply too small to establish sources. The extension of the events to large Galactic latitudes and the absence of significant event clusters suggest that a significant contribution of the signal originates

in extragalactic sources.

Given the inconclusive nature of the evidence, speculations on the origin of the cosmic neutrinos have been many. Possible source candidates include galaxies with intense star formation [47, 55, 56], cores of active galactic nuclei [57, 58], low-power  $\gamma$ -ray bursts [59, 60], intergalactic shocks, and active galaxies embedded in structured regions [55, 61].

Galactic scenarios are, however, viable and include the diffuse neutrino emission of Galactic cosmic rays [49, 62], the joint emission of Galactic PeVatrons [30, 63], and extended Galactic structures like the Fermi Bubbles [49, 64, 65] or the Galactic Halo [66]. A possible association with the sub-TeV diffuse Galactic  $\gamma$ -ray emission [67] and constraints from the non-observation from diffuse Galactic PeV  $\gamma$ -rays [49, 68], previously mentioned, have also been investigated.

More radical suggestions include PeV dark matter decay scenarios [69, 70, 71]. These remind us of the fact that we have to be prepared to be surprised and that the resolution of the origin of the observed flux represents a great discovery potential. Clearly, more events are needed to do neutrino astronomy.

## 6. From Discovery Instrument to Neutrino Telescope

The search for point sources of neutrinos has resulted in upper limits on the flux of individual Galactic and extragalactic source candidates [41, 72, 73, 74, 75, 76]. As already mentioned, it may suggest that the observed cosmic neutrinos originate from a number of relatively weak sources. It is indeed important to keep in mind that the interaction rate of a neutrino is so low that it travels unattenuated over cosmic distances through the tenuous matter and radiation backgrounds of the Universe. This makes the identification of individual point sources contributing to the IceCube flux challenging [77, 78, 79]. Even so, it is also important to realize that IceCube is capable of localizing the sources by observing multiple neutrinos originating in the same location. Not having observed neutrino clusters in the present data raises the question of how many events are required to make such a model-independent identification possible. The answer to this question suggests the construction of a next-generation detector that instruments a ten times larger volume of ice. Interestingly, this can be achieved by only doubling the number of optical sensors of the present instrument. We will return to this last point later.

Let's estimate the number of cosmic neutrinos required to detect a spatial cluster of  $m$ , or more, neutrino events from the same source. The observed cluster will most likely come from a nearby source and we can hence simplify the calculation by considering Euclidean space. The number of events  $n(r)$  from a local source at a distance  $r \leq H_0^{-1}$ , i.e., smaller than the Hubble radius, is

$$n(r) \simeq \frac{H_0}{f_{\text{sky}} 4\pi r^2 \xi_z} \times \frac{N}{\rho_0} \quad (6.1)$$

Here  $N$  is the number of events from all sources,  $\rho_0$  the density of the sources, and  $f_{\text{sky}}$  the sky coverage of the detector.  $H_0$  is the Hubble constant and  $\xi_z$  a factor that depends on the cosmological evolution of the sources. For instance, assuming that the cosmic ray sources track star formation,  $\xi_z \simeq 2.4$  [80].

As a back-of-the-envelope estimate of the required total number of events for the observation of event multiplets, we consider the contribution of the closest source expected in the FoV within

a sphere of volume  $V_1 = 1/(f_{\text{sky}}\rho_0)$ . The total number of events that we expect from this volume is given by the integral of Eq. (6.1) over  $V_1$  and yields  $m = N(V_1/V_H)^{1/3}/\xi_z$  where we introduce the Hubble volume  $V_H = 4\pi/(3H_0^3)$ . Note that  $V_H/V_1$  corresponds to the effective number of sources in the FoV. In the case of continuous sources, we arrive then at an expected total for  $m$  local events of

$$N \simeq 740 \left(\frac{m}{2}\right) \xi_{z,2.4} (f_{\text{sky}}\rho_{0,-5})^{1/3}. \quad (6.2)$$

Therefore, to observe a cluster of events from the nearest source requires a sample of 724 neutrinos for a local source density of  $\rho_0 = 10^{-5}\text{Mpc}^{-3}$ , the density of AGNs. Other source candidates may have larger or smaller densities but notice that the dependence of the number of events required on the density is relatively weak. Still, it will realistically require a sample of more than a thousand neutrino events with good angular resolution and little background to identify the sources. This would take roughly 20 years or so with the present instrument. An instrument with  $5 \sim 10$  times the sensitivity of IceCube is required to operate as an effective telescope collecting a thousand events in a few years. Detailed calculations that take into account ensemble variations of the source distribution as well as the event statistics of individual sources can be found in reference [80].

Significantly fewer events are required if the observed events are correlated to an astronomical catalogue and the sources are variable in time, typical for extragalactic sources [80]. In the case of transient sources, we have to take into account that the number of sources is increasing with observation time  $T_{\text{live}} = N/\dot{N}$ . Solving in terms of the total observation rate  $\dot{N}$  we arrive at

$$N \simeq 637 \left(\frac{m}{2}\right)^{3/2} \xi_{z,2.4}^{3/2} (f_{\text{sky}}\dot{\rho}_{0,-6}/\dot{N}_2)^{1/2}, \quad (6.3)$$

with an event rate  $\dot{N} = 100\dot{N}_2/\text{yr}$ . In the case of rare transient sources like long duration GRBs with (isotropic equivalent) rate density of  $\dot{\rho}_0 \simeq 10^{-9}\text{Mpc}^{-3}\text{yr}^{-1}$  [81], an identification of the sources with IceCube itself is still likely.

Despite the degraded resolution and the reduced potential for astronomy, the observation of electron and tau neutrinos should still be a priority. They complement the sky coverage of muon neutrinos that, at PeV energy, are mostly detected near the horizon because they are absorbed by the Earth. At high energies, neutrino production can happen in the production and decay of unstable nuclei, e.g., neutrons with  $n \rightarrow pe^- \bar{\nu}_e$ , or mesons, e.g.,  $\pi^+ \rightarrow \mu^+ \nu_\mu$ . Note that the neutrino production from the decay of muons  $\mu^+ \rightarrow e^+ \nu_e \bar{\nu}_\mu$  can be suppressed relative to the pion decay channel if synchrotron losses are important. Hence, the flavor composition is likely energy dependent and provides insight into the relative energy loss of high-energy pions and muons in the magnetic field of the cosmic accelerator [82].

Figure 9 shows the general neutrino flavor phase space  $\nu_e:\nu_\mu:\nu_\tau$  and the expected intrinsic flavor ratio in astrophysical sources from neutron decay (triangle), pion+muon decay (circle), and muon-damped pion decay (square). The observable neutrino flavor ratio is expected to be averaged over many oscillations. This leaves only a very narrow flavor composition, which is shown as the flat triangle inset in the center of Fig. 9. The corresponding observable flavor ratios of the three astrophysical production mechanisms are also indicated. The final parameter space is very close to the ‘‘tri-bi-maximal’’ approximation of mixing angles, which predicts that the final flavor ratio depends only on the initial electron neutrino ratio  $x = N_{\nu_e}/N_{\nu_{\text{tot}}}$  and  $(2/3+x):(7/6-x/2):(7/6-x/2)$ . At

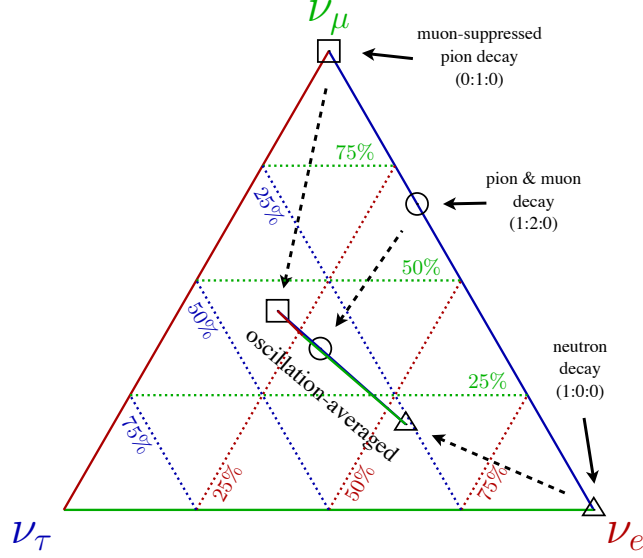


**Figure 9:** Neutrino flavor phase space after oscillation. We use the best-fit oscillation parameters  $\sin^2 \theta_{12} = 0.304$ ,  $\sin^2 \theta_{23} = 0.577$ ,  $\sin^2 \theta_{13} = 0.0219$ , and  $\delta = 251^\circ$  following Ref. [83] updated after *Neutrino 2014* [84]. Each position in the triangle parametrizes a general initial flavor ratio ( $\nu_e : \nu_\mu : \nu_\tau$ ). We also indicate specific ratios for neutron decay and pion production. The inner triangle is the corresponding observable phase space after decoherence of the neutrino flavor state over large times or distances.

sub-PeV energies (before  $\nu_\tau$  events can be distinguished from single cascades) this corresponds to an expected fraction for tracks out of the total number of events of  $7/24 - x/8$ , where we take into account that CC interactions are about three times larger than neutral current interactions at these energies. The uncertainty of the inferred intrinsic electron-neutrino fraction  $x$  is hence about eight times higher than the uncertainty of the track fraction. The situation becomes even more challenging if we include backgrounds and systematic uncertainties.

The situation improves at super-PeV neutrino energies. On one hand, the decay length of the  $\tau$  produced in CC  $\nu_\tau$  interactions becomes resolvable by the detector and can in principle be distinguished from tracks and cascade events as argued before. On the other hand, electron anti-neutrinos  $\bar{\nu}_e$  can resonantly interact with in-ice electrons via the Glashow resonance,  $\bar{\nu}_e e^- \rightarrow W^-$ , at neutrino energies of about 6.3 PeV. This could be observable as a peak in the cascade spectrum, depending on the relative contribution of  $\bar{\nu}_e$  after oscillation. In principle, this will allow us to answer the basic question of whether the cosmic neutrinos are photo- or hadro-produced in the source with different neutrino-to-anti-neutrino ratios [85].

Construction of a next-generation instrument with at least five times higher sensitivity would likely result in the observation of cosmogenic neutrinos. The rate expected with IceCube currently is only one event per year, assuming that all cosmic rays are protons (and, it is difficult to imagine that not a significant component of the highest energy neutrinos would be protons). Obviously, higher sensitivity would also benefit the wide range of measurements performed with the present detector, from the search for dark matter to the precision limits on any violation of Lorentz invariance.

By building IceCube, we were able to map the optical properties of natural ice over large distances, and we made the surprising discovery that the absorption length of the Cherenkov light to which the DOMs are sensitive exceeds 100 m. In fact, in the lower half of the detector it exceeds 200 m. Although the optical properties vary with the layered structure of the ice, the average absorption length dictates the distance by which one can space the strings of sensors without spoiling the uniformity of the detector. Modeling indicates that spacings of 250 m, possibly larger, are acceptable. One can thus sufficiently instrument a ten-times-larger volume of ice with the same number of strings used to build IceCube. The project would be free of risk since the performance of the DOMs is understood and we know how to deploy them. Furthermore, the costs are understood. Designed before 1999, all of the components of IceCube can be significantly updated for improved performance.

The larger spacings do of course result in a higher threshold but this is not necessarily bad. While the 100,000 or so atmospheric neutrinos that IceCube collects above a threshold of 100 GeV every year were useful for calibration, they represent a severe background for isolating the cosmic component of the flux. The peak sensitivity to an  $E^{-2}$  spectrum is reached at 40 TeV [86]. While the detector has to be efficient below that energy, a threshold much lower than this value introduces background without a gain in signal. Designs for a next-generation instrument are in progress.

## References

- [1] Reines, F. and Cowan, Jr., C.L., *Nature* 17 (1956) 446
- [2] Greisen, K., *Ann. Rev. Nucl. Part. Sci.* 10 (1960) 63
- [3] Reines, F., *Ann. Rev. Nucl. Part. Sci.* 10 (1960) 1
- [4] Markov, M.A., *Proc. 1960 Intl. Conf. on High Energy Physics* 578 (1960)
- [5] Gaisser, T.K., Halzen, F. and Stanev, T., *Phys. Rept.* 258 (1995) 173 Erratum 271 355, hep-ph/9410384; Learned, J.G. and Mannheim, K., *Ann. Rev. Nucl. Part. Science* 50 (2000) 679; Halzen, F. and Hooper, D., *Rep. Prog. Phys.* 65 (2002) 1025, astro-ph/0204527; Becker, J., *Phys. Rept.* 458 (2008) 173; Katz, U.F. and Spiering, C., *Prog. Part. Nucl. Phys.* 67 (2012) 651, astro-ph.HE/11110507; Halzen, F., *La Rivista del Nuovo Cimento*, 36 (2012) N3
- [6] Roberts, A., *Rev. Mod. Phys.* 64 (1992) 259
- [7] Berezhinsky, V.S. and Zatsepin, G.T., *Physics Letters B* 28 (1969) 423
- [8] Zheleznykh, I., *Int. J. Mod. Phys. A* 21S1 (2006) 1; Markov, M. and Zheleznykh, I., *Nucl. Phys.* 27 (1961) 385
- [9] Babson, J., Barish, R., Becker-Szendy, R., et al., *Phys. Rev. D* 42 (1990) 3613
- [10] Balkanov, V.A., et al. (BAIKAL Collab.), *Nucl. Phys. B Proc. Suppl.* 118 (2003) 363
- [11] Aggouras, G., et al. (NESTOR Collab.), *Astropart. Phys.* 23 (2005) 377
- [12] Aguilar, J.A., et al. (ANTARES Collab.), *Astropart. Phys.* 26 (2006) 314
- [13] Migneco, E., *J. Phys. Conf. Ser.* 136 (2008) 022048
- [14] Margiotta, A. [KM3NeT Collab.], *JINST* 9, C04020 (2014) arXiv:1408.1132 [astro-ph.IM]

- [15] IceCube Collab. PDD, available at <http://www.icecube.wisc.edu/science/publications/pdd/pdd.pdf>, (2001)
- [16] Ahrens, J., et al. (IceCube Collab.), *Astropart. Phys.* 20 (2004) 507, astro-ph/0305196
- [17] Aartsen, M.G., et al. (IceCube Collab.), *Nucl. Instrum. Meth. A* 711 (2013) 73, arXiv:1301.5361 [astro-ph.IM]
- [18] Halzen, F., *Nuovo Cimento* 36, no. 3, 81 (2013)
- [19] Beringer, J., et al. (Particle Data Group Collab.), *Phys. Rev. D* 86, 010001 (2012), §30.7
- [20] Ahrens, J., et al. (AMANDA Collab.), *Nucl. Instrum. Meth. A* 524, 169 (2004)
- [21] Aartsen, M.G., et al. (IceCube Collab.), *JINST* 9 (2014), P03009, arXiv:1311.4767
- [22] Sommers, P. and Westerhoff, S., *New J. Phys.* 11 (2009) 055004, astro-ph/08021267; A.M. Hillas (2006), astro-ph/0607109v2; and Berezhinsky, V., *J. Phys. Conf. Ser.* 120 (2008) 012001, astro-ph/08013028
- [23] Enberg, R., Reno, M.H. and Sarcevic, I., *Phys. Rev. D* 78 (2008) 043005, arXiv:0806.0418 [hep-ph]
- [24] Gonzalez-Garcia, M.C., Maltoni, M. and Rojo, J., *JHEP* 0610, 075 (2006), hep-ph/0607324
- [25] Daum, K., et al. (Frejus Collab.), *Z. Phys. C* 66, 417 (1995)
- [26] Abbasi, R., et al. (IceCube Collab.), *Phys. Rev. D* 79, 102005 (2009)
- [27] Abbasi, R., et al. (IceCube Collab.), *Astropart. Phys.* 34, 48 (2010)
- [28] Abbasi, R., et al. (IceCube Collab.), *Phys. Rev. D* 83, 012001 (2011)
- [29] Abbasi, R., et al. (IceCube Collab.), *Phys. Rev. D* 84, 082001 (2011)
- [30] Gonzalez-Garcia, M., Halzen, F., and Niro, V., *Astropart. Phys.* 57, 39 (2014), arXiv:1310.7194
- [31] Aartsen, M.G., et al. (IceCube Collab.), arXiv:1406.6757 [astro-ph.HE]
- [32] Rhode, W., et al., *Astropart. Phys.* 4 (1996) 217; Ambrosio, M., et al., *Astropart. Phys.* 19 (2003) 1, arXiv:astro-ph/0203181
- [33] Aartsen, M.G., et al. (IceCube Collab.), *Phys. Rev. Lett.* 111, 021103 (2013), arXiv:1304.5356 [astro-ph.HE]
- [34] Schukraft, A. (IceCube Collab.), *Nucl. Physics B Proc. Suppl.* (2013) 266-268, arXiv:1302.0127 [astro-ph.HE]
- [35] Aartsen, M.G., et al. (IceCube Collab.), arXiv:1312.0104 [astro-ph.HE]
- [36] Aglietta, M., et al. (LVD Collab.), *Phys. Rev. D* 60, 112001 (1999)
- [37] Schukraft, A. (IceCube Collab.), *Nucl. Phys. Proc. Suppl.* 237-238, 266 (2013), arXiv:1302.0127v2 [astro-ph.HE]
- [38] Schönert, S., Gaisser, T.K., Resconi, E. and Schulz, O., *Phys. Rev. D* 79, 043009 (2009)
- [39] Aartsen, M.G., et al. (IceCube Collab.), arXiv:1405.5303 [astro-ph.HE]
- [40] Weaver, C., Spring APS Meeting, Savannah, Georgia (2014)
- [41] Adrian-Martinez, S., et al., (ANTARES Collab.), *Astrophys. J.* 786, L5 (2014), arXiv:1402.6182 [hep-ex]
- [42] Kopper, C. (IceCube Collab.), ICRC 2013, paper 0650; Klein, S. (IceCube Collab.), ICRC 2013

- [43] Apel, W.D., et al. (The KASCADE-Grande Collab.), arXiv:1306.6283 [astro-ph.HE]
- [44] Aartsen, M.G. et al. (IceCube Collab.), Phys. Rev. D 88, 042004 (2013), arXiv:1307.3795 [astro-ph.HE]
- [45] Waxman, E. and Bahcall, J.N., Phys. Rev. D 59 (1999) 023002 [hep-ph/9807282]
- [46] Bahcall, J.N., and Waxman, E., Phys. Rev. D 64 (2001) 023002 [hep-ph/9902383]
- [47] Loeb, A. and Waxman, E., JCAP 0605, 003 (2006), astro-ph/0601695
- [48] Katz, B., Waxman, E., Thompson, T. and Loeb, A., arXiv:1311.0287 [astro-ph.HE]
- [49] Ahlers, M. and Murase, K., Phys. Rev. D 90, 023010 (2014), arXiv:1309.4077 [astro-ph.HE]
- [50] Matthews, J., et al. (UTAH Collab.), Astrophys. J. 375, 202 (1991)
- [51] Chantell, M.C., et al. (CASA-MIA Collab.), Phys. Rev. Lett. 79, 1805 (1997), arXiv:astro-ph/9705246
- [52] Schatz, G., et al. (KASCADE Collab.), Proceedings of the 28th ICRC, Tsukuba, Japan (2003)
- [53] Aartsen, M.G., et al. (IceCube Collab.), Phys. Rev. D 87, 062002 (2013), arXiv:1210.7992 [astro-ph.HE]
- [54] Abdo, A.A., et al. (Fermi-LAT Collab.), Phys. Rev. Lett. 104 (2010) 101101, arXiv:1002.3603 [astro-ph.HE]
- [55] Murase, K., Ahlers, M. and Lacki, B.C., Phys. Rev. D 88 (2013) 121301(R), arXiv:1306.3417 [astro-ph.HE]
- [56] He, H.-N., Wang, T., Fan, Y.-Z., Liu, S.-M. and Wei, D.-M., arXiv:1303.1253 [astro-ph.HE]
- [57] Stecker, F.W., Done, C., Salamon, M.H. and Sommers, P., Phys. Rev. Lett. 66, 2697 (1991)
- [58] Stecker, F.W., Phys. Rev. D 88, 047301 (2013), arXiv:1305.7404 [astro-ph.HE]
- [59] Waxman, E. and Bahcall, J.N., Phys. Rev. Lett 78, 2292 (1997), astro-ph/9701231
- [60] Murase, K. and Ioka, K., Phys. Rev. Lett. 111, 121102 (2013), arXiv:1306.2274 [astro-ph.HE]
- [61] Blasi, P. and Ptuskin, V., Astrophys. J. 487, 529 (1997), astro-ph/9609048
- [62] Kachelriess, M. and Ostapchenko, S., Phys. Rev. D 90, 083002 (2014), arXiv:1405.3797
- [63] Fox, D.B., Kashiyama, K., and Meszaros, P., Astrophys. J., 774, 74 (2013), arXiv:1305.6606 [astro-ph.HE]
- [64] Razzaque, S., Phys. Rev. D 88, 081302 (2013), arXiv:1309.2756
- [65] Lunardini, C., Razzaque, S., Theodosiou, K.T. and Yang, L., (2013), arXiv:1311.7188
- [66] Taylor, A.M., Gabici, S. and Aharonian, F., (2014), arXiv:1403.3206
- [67] Neronov, A., Semikoz, D.V. and Tchernin, C., Phys. Rev. D 89, 103002 (2014), arXiv:1307.2158 [astro-ph.HE]
- [68] Gupta, N., Astropart. Phys. 48, 75 (2013), arXiv:1305.4123
- [69] Feldstein, B., Kusenko, A., Matsumoto, S. and Yanagida, T.T., Phys. Rev. D 88, 015004 (2013), arXiv:1303.7320 [hep-ph]
- [70] Esmaili, A. and Serpico, P.D., JCAP 1311 (2013) 054, arXiv:1308.1105 [hep-ph]
- [71] Bai, Y., Lu, R. and Salvado, J., (2013), arXiv:1311.5864

- [72] Abbasi, R., et al., (IceCube Collab.), *Astrophys. J.* 744 1 (2012), arXiv:1104.0075
- [73] Adrian-Martinez, S., et al. (ANTARES Collab.), *Astrophys. J.* 760 53 (2012), arXiv:1207.3105
- [74] Abbasi, R., et al. (IceCube Collab.), *Nature* 484, 351 (2012), arXiv:1204.4219
- [75] Aartsen, M., et al. (IceCube Collab.), *Astrophys. J.* 779, 132 (2013), arXiv:1307.6669
- [76] Adrian-Martinez, S., et al. (ANTARES Collab.), *A&A* 559, 9 (2013), arXiv:1307.0304
- [77] Lipari, P., *Nucl. Instrum. Meth. A* 567, 405 (2006) [astro-ph/0605535]
- [78] Becker, J.K., Rhode, W., Biermann, P.L. and Muenich, K., *Astropart. Phys.* 28, 98 (2008) [astro-ph/0607427]
- [79] Silvestri, A. and Barwick, S.W., *Phys. Rev. D* 81, 023001 (2010), arXiv:0908.4266 [astro-ph.HE]
- [80] Ahlers, M. and Halzen, F., arXiv:1406.2160 [astro-ph.HE]
- [81] Wanderman, D. and Piran, T., *Mon. Not. Roy. Astron. Soc.* 406, 1944 (2010), arXiv:0912.0709 [astro-ph.HE]
- [82] Kashti, T. and Waxman, E., *Phys. Rev. Lett.* 95, 181101 (2005) [astro-ph/0507599]
- [83] Gonzalez-Garcia, M.C., Maltoni, M., Salvado, J. and Schwetz, T., *JHEP* 1212, 123 (2012), arXiv:1209.3023 [hep-ph]
- [84] <http://www.nu-fit.org>
- [85] Anchordoqui, L.A., Goldberg, H., Halzen, F. and Weiler, T.J., *Phys. Lett. B* 621, 18 (2005) [hep-ph/0410003]
- [86] Halzen, F., Kappes, A. and O’Murchadha, A., *Phys. Rev. D* 78, 063004 (2008), arXiv:0803.0314 [astro-ph]